The Effect of the Packing Parameters, Gate Geometry, and Mold Elasticity on the Final Dimensions of a Molded Part

V. LEO *and* CH. CUVELLIEZ*

Solvay Research & Technology
1120 Brussels, Belgium

Despite a significant number of publications and the increasing use of numerical simulation, there is still a debate about the optimum gate design and packing conditions in the molding industry. Shrinkage uniformity for unfilled polymers is dominated by the time dependent pressure distribution in the cavity and the resulting volumetric shrinkage; gate freeze-off is obviously important and difficult to predict; and pressure gradients during the packing phase, depend on process and design parameters and are also affected by the mold elasticity. Molding trials have been conducted on an instrumented mold (fan gated rectangular slab, 2 mm thick) under a variety of processing conditions and with different gate thicknesses using HDPE (Solvay Eltex A1050). Pressure decay during the molding cycle at different locations along the flow path have been correlated with sample thickness distribution. Overpacking at moderate packing pressure is shown to be a direct consequence of mold elasticity and to be related to both filling flow rate and gate thickness. The decay to a finite residual pressure can be computed by coupling the mold elasticity with the PVT behavior of the polymer. The results highlight the importance of gate design and processing parameters on the dimensional accuracy of the part and low internal stress level. When dealing with thick gates, packing pressure profiling appears to be the best way to avoid gate area overpacking. Mold elastic deformation can play a significant role in the cavity pressure-time history, even for a seemingly stiff mold construction.

INTRODUCTION

Injection molding is a major process in the plastic industry accounting for the largest volume of thermoplastic parts production (1). The melt is delivered at high flow rate into the cavity, usually through a gate restriction. Immediately after filling, a pressure controlled phase ensures shrinkage compensation in order to optimize part dimensions. Maintaining the dimensional accuracy of the final part is critical for technical applications.

Obviously, proper packing will reduce volumetric shrinkage and the linear shrinkage itself, yielding parts with dimensions closer to those of the cavity. However, lower shrinkage is sometimes obtained as a trade-off for other properties, i.e., internal stress level or warpage due to uneven shrinkage.

From the scientific point of view the packing phase is also a challenging exercise. The process is highly transient and it involves complex thermodynamics as well as a highly compressible flow situation. Difficult morphological issues further complicate the picture when one is dealing with semicrystalline polymers.

Literature is available on flow simulation, including, in the last ten years or so, many papers on the packing phase. For a comprehensive introduction refer to Chung (2) and Chiang (3).

Our initial goal, when designing and using the instrumented mold described in this paper, was to validate the pressure predictions of commercially available simulation code, essentially in the filling phase. Interesting results have been obtained with the setup (mainly unpublished work) and have shown some of the weaknesses of the numerical approach. More recently, with the development of packing simulation, we decided to specifically validate the packing phase by monitoring cavity pressure tranducers along the flow in a variety of molding conditions.

Our first trials immediately showed some significant and peculiar deviations of the simulation from the experimental results. It appeared that overpacking was consistently achieved experimentally at packing

* Current address: A.V.N., Av. du Roi 157, 1160 Brussels, Belgium.

conditions (especially pressure levels), which, according to the numerical analysis, should not have produced low or negative shrinkages. Overpacking has often been observed and sometimes discussed in the literature (3–6). Although technically unacceptable (demolding problems), negative shrinkages can readily be obtained in some cavities if excessive pressure is applied for a sufficient time during the holding phase. The thermodynamical behavior of the polymer, best seen in the PVT diagrams, clearly indicates the possibility of achieving overpacking at pressure levels compatible with the available molding machinery.

We found that the observed overpacking at relatively modest pressure levels is a direct consequence of the mold elastic deformability. The effect of such a behavior is similar to what is achieved with patented *active* mold technology, using spring action (7) or hydraulic control (8). When the packing is *assisted* in this way the pressure in the cavity is much more uniform during the holding phase and this produces parts with more uniform shrinkage and lower stress or birefringence levels (9–11). For a centrally gated part this could dramatically reduce the typical warpage problems associated with the differential shrinkage and the decreasing efficiency of the packing phase away from the gate (12).

To assess the importance of mold deformability we added a strain gage to the setup and monitored the flexural strain of the mold backplate in all our experiments (13). The deflection and cavity pressure observations have been found to agree with a simple model of the holding phase including an elastic volumetric expansion of the cavity under pressure.

The full experiment includes a study of the gate thickness influence on the packing efficiency. Part weight and thickness along the flow direction have been measured for all geometries and processing conditions. Reduced gate thickness or proper packing pressure profiling appear to be of utmost importance in the quest of a low-stress/uniform shrinkage part.

EXPERIMENTAL SETUP

The injection molding experiments were performed on a Netstal N350/150 MP 150 ton machine with a 40 mm diameter barrel. This clamping capacity should theoretically stand >200 MPa uniform pressure in the cavity described below. This overcapacity was necessary to minimize the risk of dimensional instability of the samples due to mold opening.

The mold cavity is a rectangular slab, 150 × 40 × 2 mm, gated through an end fan-gate of 0.5, 1 or 2 mm thicknesses, as shown in *Fig. 1*. The cavity is equipped with three Kistler 6157 AO4 piezoelectric pressure tranducers read by Kistler 5089C charge amplifiers. The steel backplate of the mold on the moving side is equipped with a strain gauge monitoring the mold elastic flexural deformation.

Internal pressure signals and some machine parameters (hydraulic pressure and screw velocity) were sampled at a typical rate of 50 Hz/channel through a 16-channel AD converter. The data was handled on a Quadra 950 Macintosh using internally developed code based on Labview release 2.2.1 virtual instruments library and language.

The material used for the experiment is an HDPE from Solvay, Eltex A1050 (Mn 15,000, Mw 105,000, Mz 600, MFI(2.16 kg) 5 g/min at 190°C). This material has already been extensively characterized for round robin trials or numerical simulation validation (Moldflow Australia, AC Technology USA, RAPRA UK, SWO Germany, Solvay Belgium, etc.).

The mold was at 40°C and the melt temperature 200°C. Parts were molded at three different ram speeds: 5, 10 and 50 mm/s. Lower rates were eliminated because of unstable flow through the thin 0.5 mm gate or unacceptable backflow. At each speed, ram position was adjusted to produce a shortshot (~95% full) at the switchover to packing pressure (position triggered switchover). Packing pressure was varied from 40 MPa to >110 MPa (nominal melt pres-

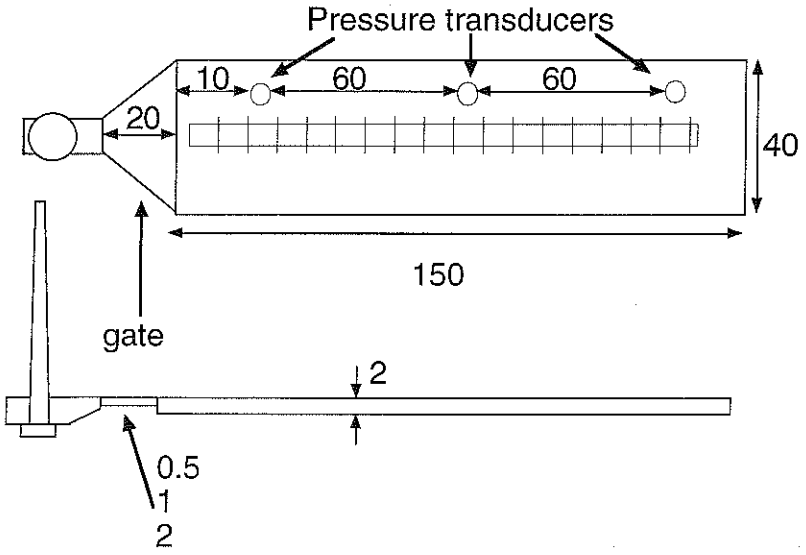

Fig. 1. Geometry of the instrumented mold. Dimensions in mm. Note the variable thickness fan gate.

Table 1. List of Processing Conditions.

Fill Rate (mm/s)	Gate (mm)	Packing Pressure (Bar)								
5	2	400	500	600	700		800			
	1	500				750		1000		1200
	0.5	500					800	1000	1100	1200
10	2	400		600			800			
	1	500				750		1000		1200
	0.5	500					800		1100	1200
50	2	400		600			800			
	1	500				750		1000		1200
	0.5	500					800		1100	

Highlighted packing pressures correspond to observed residual pressure at end of cycle.

sure) for each gate configuration and each filling flow rate. A packing time scan was performed at 5 mm/s fi" rate and 80 MPa packing pressure for each gate t.. kness.

Five samples were kept for each molding condition after reaching sufficient repeatability. Manual ejection was necessary because the strain gauge prohibited the use of the ejector plate mechanism.

Sample weight was measured with and without the sprue and averaged over the five samples. Sample thickness was measured on a table spring loaded Mitutoyo 7323 micrometer (≈0.005 mm repeatability) at seven locations aligned along the flow direction. End of flow frozen skin thickness at three positions (pressure transducers) was measured by observing microtomed sections under crosspolarized filters for two distinct sample orientations (to rule out visual errors due to stress induced fringes).

Table 1 summarizes the investigated processing conditions (optimized packing time of 15 sec). As seen, different packing pressures were used for the various gate thicknesses. Pressures were actually adjusted according to gate pressure drop to ensure proper ob- s ation of the transition to overpacking to be discussed later (residual pressure at end of cycle, typical of overpacking, was observed at the processing conditions highlighted in *Table 1*). Identical pressure would not have been of particular interest, as these nominal values would produce different melt pressures through the different gates, anyway.

RESULTS

Packing Time Scan

The aim of the experiment was to accurately assess freeze-off time of the gate and to follow the thickness distribution buildup as the packing time was increased. *Figure 2* shows the part (runnerless) weight as a function of packing time for a given packing pressure and fill rate for the three gate dimensions. The leveling off of the curves relates to the freezing of the gate or the part if the gate freezes later than the part (14). Once the weight has reached this level, the packing flow rate has vanished and any additional packing is useless (a few extra seconds might actually be necessary to prevent the pressurized melt to burst back through the "just frozen" gate).

Classically, in a static approximation, one would expect the freezing time (calculated from the end of fill) to be roughly proportional to the square of the thickness. A Moldflow simulation approximates this:

2 mm gate . . . 15 s
1 mm gate . . . 4 s
0.5 mm gate . . . 1 s

Experimental results, as seen in *Fig. 2*, are definitely less than linearly related to the thickness. The

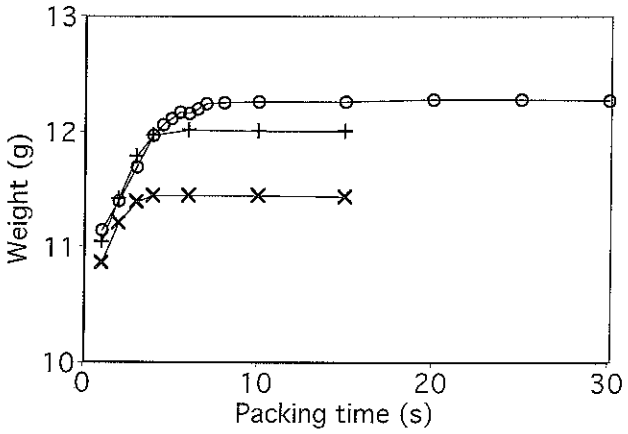

Fig. 2. Runnerless part weight as a function of packing time at 5 mm/s ram speed and 80 MPa packing pressure. (○) 2 mm gate, (+) 1 mm gate, (×) 0.5 mm gate.

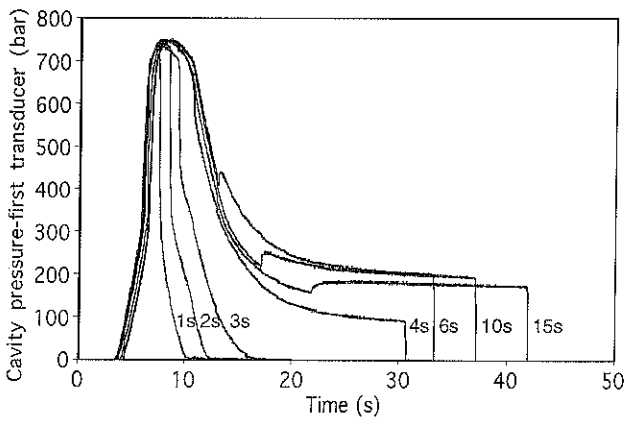

Fig. 3. Time-pressure plot of the first transducer (close to the gate) for different packing times reported on the graph. Fill rate is 5 mm/s and nominal packing pressure 100 MPa.

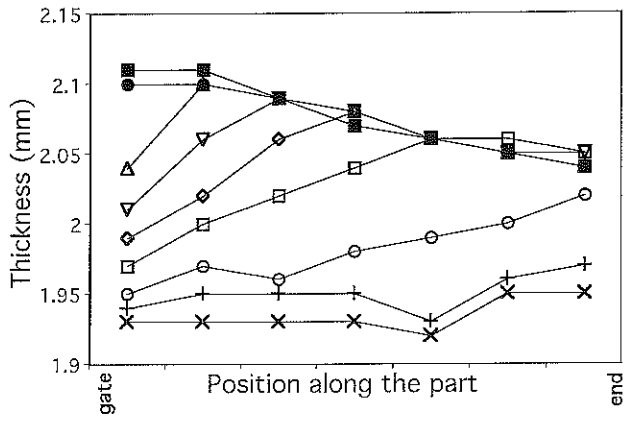

(a)

Fig. 4a. Thickness distribution along the part as a function of packing time at 5 mm/s fill rate and nominal 80 MPa packing pressure. Gate thickness is 2 mm. (×) 1 s, (+) 2 s, (○) 3 s, (□) 4 s, (◇) 4.5 s, (△) 5 s, (▽) 6 s, (●) 10 s, (■) 30 s.

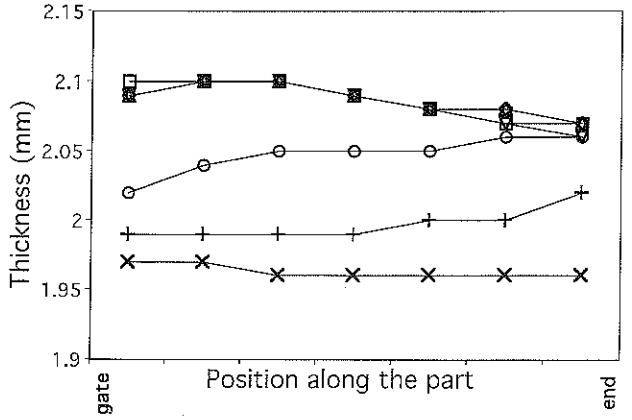

(b)

Fig. 4b. Thickness distribution along the part as a function of packing time at 5 mm/s fill rate and nominal 100 MPa packing pressure. Gate thickness is 1 mm. (×) 1 s, (+) 2 s, (○) 3 s, (□) 4 s, (◇) 6 s, (▽) 10 s, (△) 15 s.

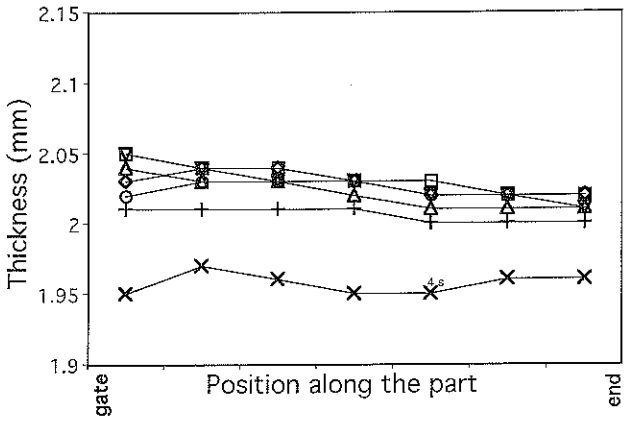

(c)

Fig. 4c. Thickness distribution along the part as a function of packing time at 5 mm/s fill rate and nominal 100 MPa packing pressure. Gate thickness is 0.5 mm. (×) 1 s, (+) 2 s, (○) 3 s, (□) 6 s, (◇) 10 s, (▽) 15 s.

freeze-off of the gates can also be observed on the pressure traces measured by the transducers in the cavity (*Fig. 3*). Indeed, when releasing the machine pressure, the first transducer trace clearly shows a sudden decay, due to backflow, for packing times shorter than the freezing time. For a sufficiently long packing time, this abrupt internal pressure drop upon hold release disappears. An additional small discontinuity (a slight jump up in internal pressure) is also present but does not relate to melt backflow from the cavity. It seems to originate from a mechanical effect due to mold/plates elasticity and the force exerted by the injection unit on the mold when pressure is applied. This has been observed before (4).

We measured the thickness distribution of the samples along the flow path, which, for an unfilled and low viscosity material (showing little molecular orientation), is a reasonable assessment of local packing efficiency and corresponding shrinkage. *Figures 4a–4c* clearly show the effect of gate thickness on the shrinkage distribution along the flow direction.

The buildup of the final thickness distribution is also of great interest. The 2 mm gate is actually representative of a direct sprue situation as the part is itself 2 mm thick. Many parts are molded this way, especially when using viscous materials. The results in *Fig. 4a* clearly indicate that dimensional buildup occurs first at the end of flow, which shows less shrinkage that the front area for short packing times. This is due to the significant backflow occurring in this case when the pressure is released, as already seen in the weight curve of *Fig. 2*.

As the packing time approaches the optimum value, the part maximum thickness location gradually reaches the gate area. At this stage, the part shows a decreasing thickness profile from the gate to the end of flow. The gate area is overpacked with respect to the end of flow; and even at lower packing pressures it's thickness profile is virtually unaffected.

As seen in *Fig. 4b* and 4c, a thinner gate gives a higher average shrinkage for approximately the same applied pressure. However, even for packing times shorter than the gate freeze-off time, the thickness distribution is almost flat. A trend similar, but much less severe, to the gate area overpacking seen before, also appears for the 1 mm thick gate.

Constant Packing Time

In the following, the packing time has been set to 15 sec, regardless of the gate geometry or the other processing parameters. Using this sufficiently long packing time, we have looked at the dimensional profiles of the samples, for each gate thickness and fill rate, as a function of the applied packing pressure.

Figures 5a–5c show the thickness distribution along the part, at 5 mm/s ram speed, as a function of applied packing pressure for each gate geometry. Some experiments were eliminated because of a short-shot condition (low packing pressure with a thin gate) or excessive flash (high packing pressures, especially

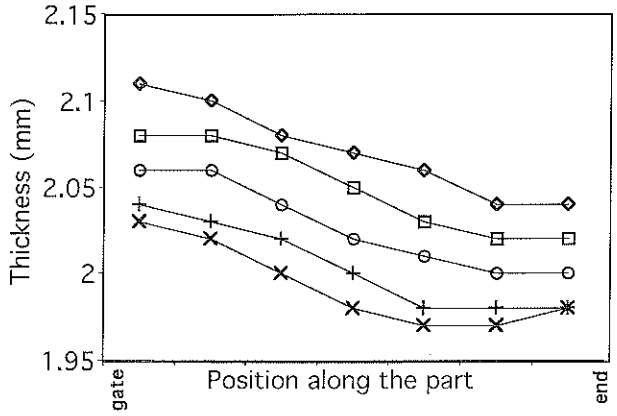

(a)

F 5a. Thickness distribution along the part as a function of p. .ing pressure at 5 mm/s fill rate and 15 s packing time. Gate thickness is 2 mm. (×) 400 bar, (+) 500 bar, (○) 600 bar, (□) 700 bar, (◇) 800 bar.

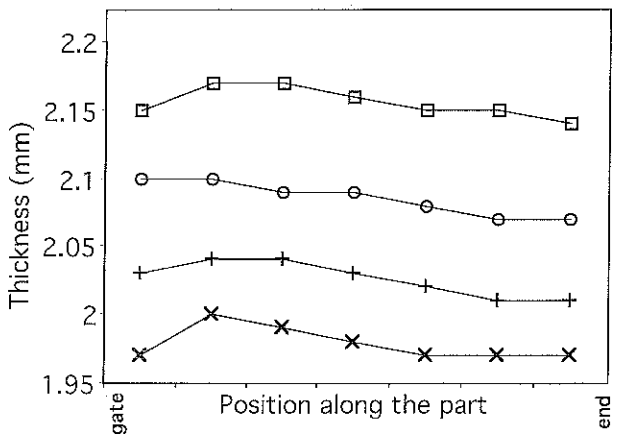

(b)

F 5b. Thickness distribution along the part as a function of packing pressure at 5 mm/s fill rate and 15 s packing time. Gate thickness is 1 mm. (×) 500 bar, (+) 750 bar, (○) 1000 bar, (□) 1200 bar.

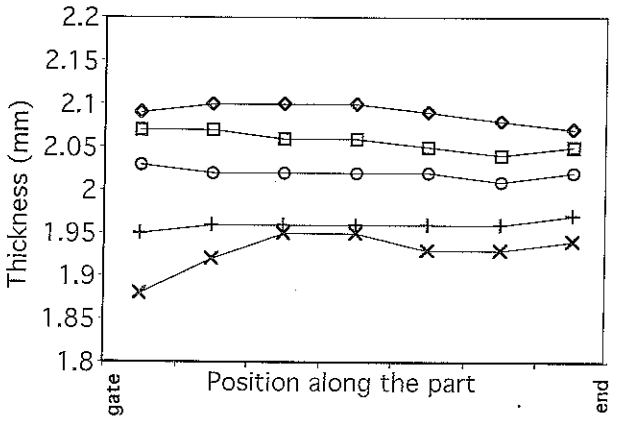

(c)

Fig. 5c. Thickness distribution along the part as a function of packing pressure at 5 mm/s fill rate and 15 s packing time. Gate thickness is 0.5 mm. (×) 500 bar, (+) 800 bar, (○) 1000 bar, (□) 1100 bar, (◇) 1200 bar.

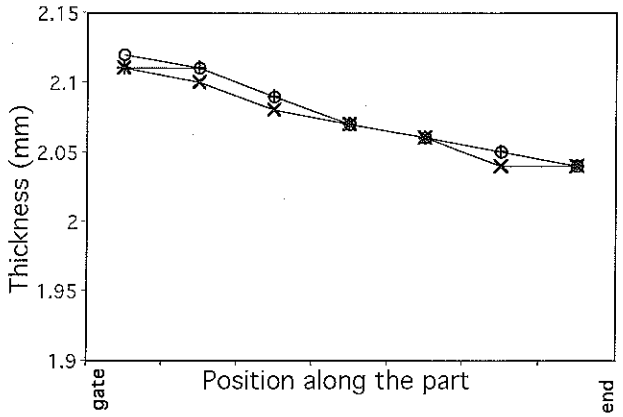

(a)

Fig. 6a. Thickness distribution along the part as a function of fill rate at 800 bar packing pressure and 15 s packing time. Gate thickness is 2 mm. (×) 5 mm/s, (+) 10 mm/s, (○) 50 mm/s.

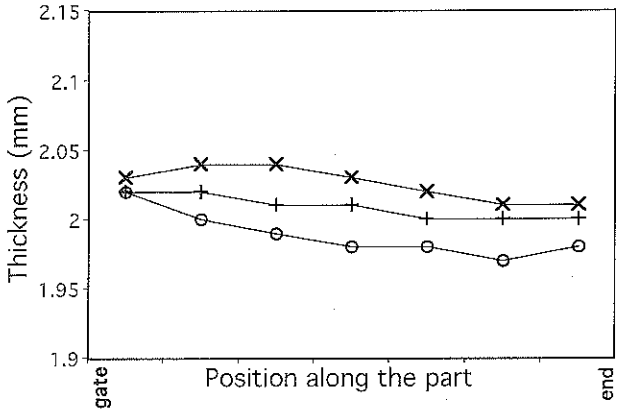

(b)

Fig. 6b. Thickness distribution along the part as a function of fill rate at 750 bar packing pressure and 15 s packing time. Gate thickness is 1 mm. (×) 5 mm/s, (+) 10 mm/s, (○) 50 mm/s.

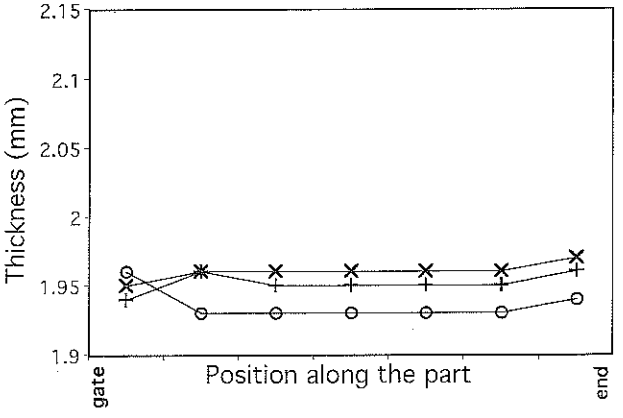

(c)

Fig. 6c. Thickness distribution along the part as a function of fill rate at 800 bar packing pressure and 15 s packing time. Gate thickness is 0.5 mm. (×) 5 mm/s, (+) 10 mm/s, (○) 50 mm/s.

with a thick gate). For a 2 mm gate, the average shrinkage increases when lowering the packing pressure, but the slope of the thickness profile is not affected. For the 0.5 and 1 mm gates, the profiles are mostly flat, and only the average thickness increases with the packing pressure.

If we select a given packing level and look at the effect of the filling rate on the thickness profile, the most striking effect is that with a 2 mm thick gate this profile is totally unaffected by the filling rate (*Fig. 6a*). On the contrary, in *Fig. 6b* and *6c*, one can see that for thinner gates the packing efficiency and the dimensional profile are related to the filling rate. A higher filling rate gives a higher shrinkage.

Pressure Traces Inside the Cavity

Figures 7a–7c show typical pressure traces inside the cavity for the 50 mm/s ram speed and ~80 MPa applied packing pressure. Again, the thick gate shows a drastically different behavior. The pressure gradients between the transducers are very significant. Ambient pressure is reached promptly and almost simultaneously by the transducers for the 0.5 and the 1 mm gate.

In the case of the thick gate, pressure decay is much slower, and the first transducer (closer to the gate) decays to a finite residual pressure of ~25 MPa. The peak packing pressure seen by the first transducer for a given nominal value is a function of the gate thickness and of the filling rate (*Table 2*). Some of these values have been interpolated from adjacent experimental data. The curves in *Figs. 7a–7c* also show the mold deflection as recorded by the strain gauge. This signal roughly follows the pressure traces, showing a maximum mold deflection when the internal pressure peaks at the beginning of the packing cycle. In the case of the 2 mm gate, the decay to a nonvanishing internal pressure is reflected in the strain-gauge signal, which shows a "permanent" mold deformation. Order of magnitude of the mold deflection was checked by an analytical estimate as it will be shown in the following discussion.

Figure 8a shows the pressure traces obtained when a step programmed hydraulic pressure is used in the packing phase to minimize the pressure gradients in the part, with respect to the thick 2 mm gate. Although only five steps were available on the machine, the results, in terms of thickness distribution, are notable (*Fig. 8b*).

Frozen Skin

Most of the observed effects, including the deviations between experimental results and numerical simulations, are related to the frozen skin thickness distribution in the samples at the instant of fill. Direct measurements are difficult to perform and would mostly rely on heavier instrumentation of the mold for instance with ultrasonic transducers (8). A reasonable picture for a semicrystalline material can be obtained by optical microscopy of microtomed sections under

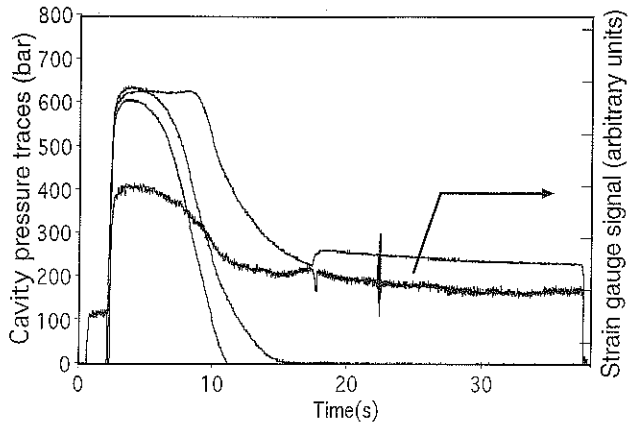

(a)

Fig. 7a. Cavity pressure traces and strain gauge signal. Fill rate 50 mm/s, packing pressure 800 bar, and packing time 15 s. Gate thickness is 2 mm. The spike at 22 s is noise.

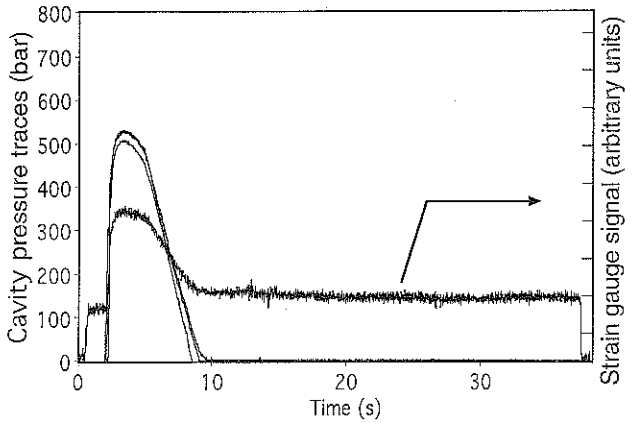

(b)

Fig. 7b. Cavity pressure traces and strain gauge signal. Fill rate 50 mm/s, packing pressure 750 bar, and packing time 15 s. Gate thickness is 1 mm.

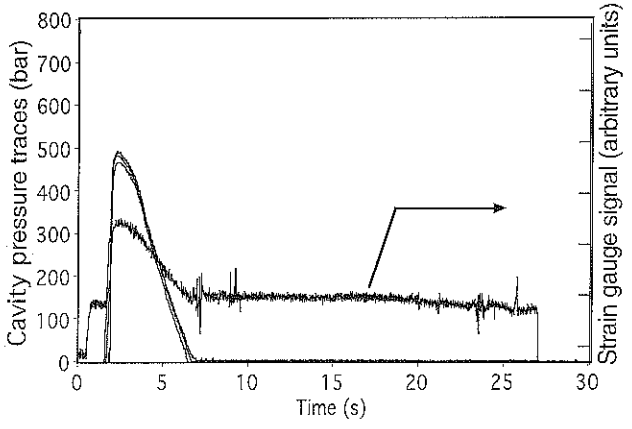

(c)

Fig. 7c. Cavity pressure traces and strain gauge signal. Fill rate 50 mm/s, packing pressure 800 bar, and packing time 15 s. Gate thickness is 0.5 mm.

Table 2a. Frozen Skin at Fill Time for a 2 mm Thick Gate.

Gate (mm)	Fill Rate (mm/s)	Packing Pressure (bar)	Frozen Skin (%)	
			Experiment	Moldflow Prediction
2	5	700	33	31
			29	41
			23	31
	10	800	23	24
			19	28
			13	19
	50	800	9	9
			8	9
			5	6

Table 2b. Frozen Skin at Fill Time for a 1 mm Thick Gate.

Gate (mm)	Fill Rate (mm/s)	Packing Pressure (bar)	Frozen Skin (%)	
			Experiment	Moldflow Prediction
1	5	750	32	36
			29	47
			23	34
	10	750	24	25
			20	30
			15	20
	50	750	11	8
			8	9
			6	6

Table 2c. Frozen Skin at Fill Time for a 0.5 mm Thick Gate.

Gate (mm)	Fill Rate (mm/s)	Packing Pressure (bar)	Frozen Skin (%)	
			Experiment	Moldflow Prediction
0.5	5	800	30	37
			26	46
			23	34
	10	800	25	28
			20	33
			14	21
	50	800	11	7
			10	9
			6	6

crosspolarized filters (15). The assumption is that the dramatic discontinuity in flow and thermodynamic history at the frozen skin boundary will show up as a clear morphological transition. Experimental results seem to back up this interpretation.

Figures 9a and *9b* show the typical difference in frozen skin thickness for a fast and slow filling rate. In *Table 2* we report the skin thickness as measured and predicted by MFL Release 8 (Moldflow) on the various experiments at three locations along the path (at the pressure transducer locations). Simulation results show the well-known non-monotonic trend. Our measurement, monotonically decreasing, seem to show that the maximum occurs before the first transducer location. A very flat maximum is expected much less than halfway downstream (dominant diffusion case) (16).

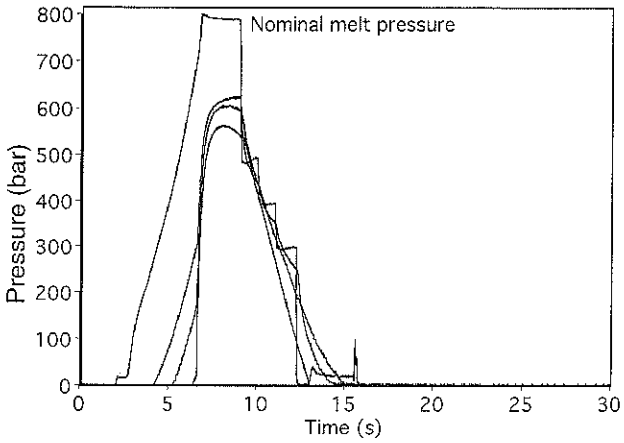

(a)

Fig. 8a. Cavity pressure traces and nominal melt pressure (hydraulic pressure) for a step profiled packing phase. Fill rate is 5 mm/s. Gate thickness is 2 mm.

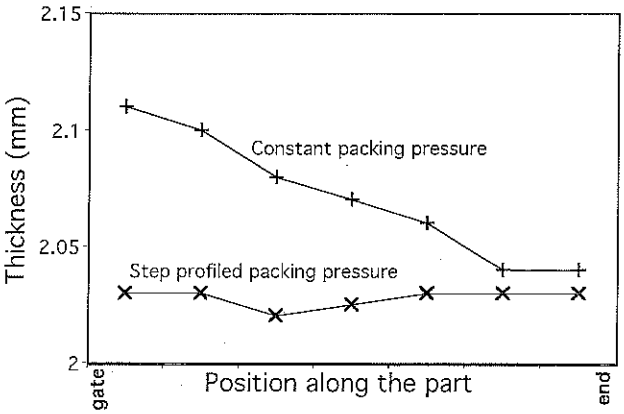

(b)

Fig. 8b. Comparative thickness distribution along the part for a constant packing pressure and the step profiled packing pressure of Fig. 8a. Fill rate 5 mm/s. Gate thickness is 2 mm.

GENERAL DISCUSSION

Most of the experimental evidence for this work has been published elsewhere. Only partial results can be found in any single paper on this subject. Our main objective was to conduct a large experiment and get a general picture of the effects of gate geometry, packing parameters, and mold elasticity on the dimensional quality of the part.

Packing "Shortshots"

The packing time scan results have clearly indicated that static based predictions of freezing times are dangerous when dealing with gates (17). The optimization of the packing time by means of the weight build up of the runnerless part is essential and should be systematically used on the floor shop. Weight

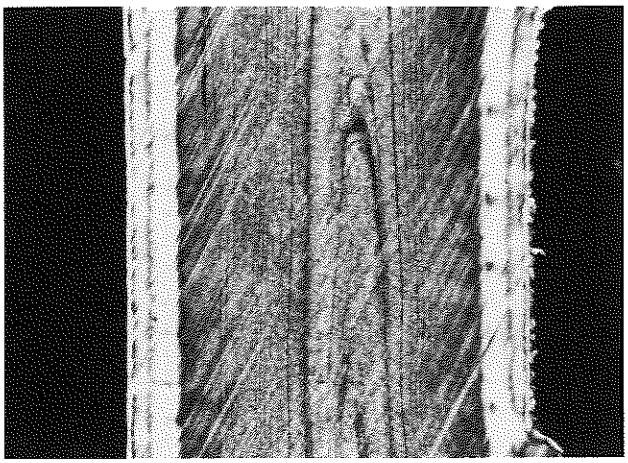

(a)

Fig. 9a. Frozen skin as seen in a microtomed section under crosspolarized filters. Fill rate 5 mm/s.

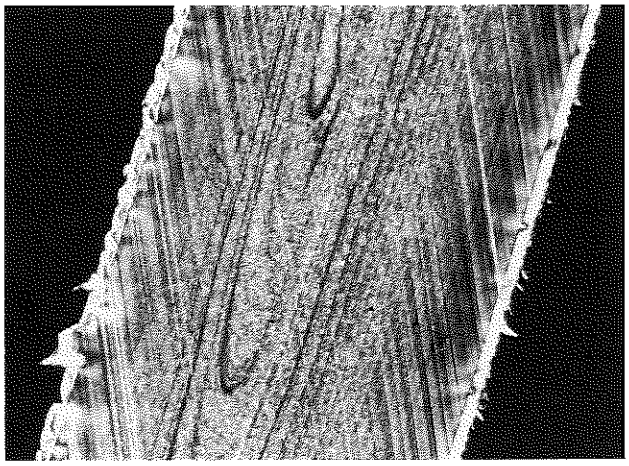

(b)

Fig. 9b. Frozen skin as seen in a microtomed section under crosspolarized filters. Fill rate 50 mm/s.

curves obtained on our sample with the sprue attached show an additional mass build up extending to about 25 sec. This, of course, merely reflects the (useless) packing of the sprue and should be disregarded when defining the proper packing time.

Internal pressure traces (see *Fig. 3* for instance) and the nonuniform thickness of the samples molded with a thick gate (*Fig. 4a*) clearly show the freezing time lag of the gate area compared to the end of flow region. This is a direct consequence of the compressibility of the melt and the heat convected during the packing flow.

Effect of Packing Pressure and Gate Thickness on the Shrinkage

Thickness measurements, much easier to perform than linear shrinkage measurements, have been assumed to reflect the local volumetric shrinkage. The higher packing level of the gate area shows up very clearly when using a thick gate. The packing flow is not interrupted by thermal gate sealing and runs until total freeze-off of the part or pressure release (whichever occurs first). This actually produces high pressure gradients along the part, creating high internal stresses upon cooling. For an amorphous polymer it would show up as a high birefringence (18). There are reports (9, 10) on the dominant effect of internal pressure history on internal stresses in molded parts. The observed gradients in the case of the thick gate (*Fig. 7a*) are also responsible for the shrinkage distribution seen in *Fig. 4a* and *5a* (decreasing from gate to end of flow).

Clearly, with a constant packing pressure and a thick gate, there is no way to make a part with uniform shrinkage. In a complex "real life" geometry this variable shrinkage can cause significant warpage of the part (12). The only advantage of the "gateless" configuration is a more efficient transmission of the pressure in the cavity for a given nominal pressure, as well as a negligible effect of the flow rate on packing efficiency, as seen in *Table 2*. As seen, despite the quasi-hydrostatic character of the holding phase, there are significant pressure drops, particularly in the feeding system. Some of these pressure drops are certainly related to the viscoelastic character of the melt and the abrupt change of thickness or flow direction (19) in the feeding system. With a thin gate we need more nominal pressure to obtain a given pressure level inside the cavity. However the packing pressure itself is rarely a process limitation (clamping force requirements will usually be more stringent). If a direct sprue is used, programming a decreasing packing pressure is the best way to overcome the drawbacks of this gating solution, as seen in *Fig. 8*.

Internal pressure measurements will greatly help to reach an optimum setting faster and more accurately than by trial and error. Adjusting the step programming for minimum pressure gradients produces a uniform shrinkage distribution. This is basically an emulation of the thin gate configuration (we let the excess material escape, with a thin gate it just does not come in). Another efficient way is to use a mechanically or hydraulically triggered valve gate. Here the user would benefit from an additional adjustable parameter (shutoff time) to optimize the shrinkage distribution.

The thickness profile results in *Fig. 5*, for an optimized packing time (15 s) are quite self-explanatory.

In the case of a thin gate (0.5 mm) the fillrate affects the average shrinkage [contrary to what has been reported (20)]. The packing flow is interrupted by the early freeze-off of the gate. Therefore, the initial mass content at switchover to packing (i.e. at the end of filltime) shows up in the final part weight. It is well known that "packless" parts are much heavier at low fill rate because of the much thicker frozen skin (higher density than the melt) at filltime (*Fig. 9*). With a thick gate (2 mm) there is no premature termination of the packing flow, which totally removes the fillrate/frozen skin effect on the final shrinkage. Thermal sealing of the gate also accounts for the decreasing average shrinkage with increasing gate dimensions. Shear heating effects are second order corrections here.

When looking at the thickness distribution along the flow, the most striking result is the sloped profile obtained with a thick gate. Thinner gates give a good constant thickness. This is in good agreement with the much lower pressure gradients developing in the part. Internal pressure and stress relaxation can also freely occur once the gate is frozen, if a significant core section is still molten. The best combination would then be a fast filling followed by a high packing pressure with a fast gate freezing time (or shutoff valve).

Overpacking and Mold Elasticity

Residual pressure at the end of cycle has been observed in a number of molding conditions, as seen in *Table 1*. Strictly speaking, overpacking occurs when the part dimensions exceed the cavity dimensions, which can also be described as a negative shrinkage situation. This is perfectly acceptable from the physical standpoint, and is easily visualized on a PVT diagram (*Fig. 10*). The packing process can be idealized and represented as a particular path on this graph.

As seen in *Fig. 10* (path II), if sufficient initial packing pressure is applied and if gate freeze off is not too rapid, the final shrinkage can be negative. When opening the mold and ejecting the part, it will expand to its final dimensions (larger than the cavity dimension). In industrial applications a negative shrinkage will usually be unacceptable as it will induce severe problems (ejection i.e.). Based on freezing temperature of HDPE and on the PVT curves, we did not expect overpacking to occur at nominal pressures much lower than 100–150 MPa (even with a thick gate and long packing time combination).

Experimentally, we found overpacking at applied pressures as low as nominal 60 MPa for the 2 mm gate thickness. The gate is important on a twofold basis. Thicker gate produces less pressure drop during the packing flow (*Table 2*) and also extends significantly the duration of this compensating flow.

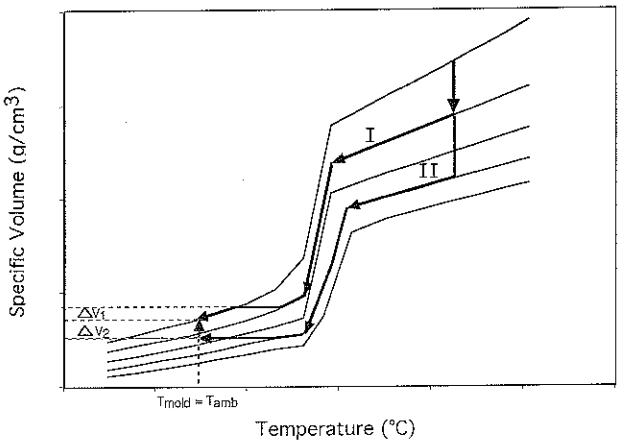

Fig. 10. Schematic PVT diagram of HDPE. Thick-line path I gives a final positive volumetric shrinkage ΔV_1, path II at high packing pressure yields a negative volumetric shrinkage ΔV_2. For clarity, the mold has been assumed to be at ambient temperature.

But this does not explain our observations. We found that the dominant effect on this "low pressure" overpacking is the mold elasticity. In the technical literature on pressure Kistler transducers (21), the existence of a finite residual internal pressure at the end of the molding cycle, is described as the result of a late switchover from filling to packing. This is not totally correct. We found that several distinct problems can arise which relate to "excessive" packing. These can be clearly classified when monitoring both internal pressure and mold deflection, as we did.

As seen on the experimental traces, the mold is elastically deformed in all cases, when sufficient internal pressure is present. This deformation will usually relax, following the trend of the internal pressure. When flash occurs (mold opening due to an unsufficient clamp force, or mold deformation itself), the mold will retain a permanent deflection, but not necessarily a permanent finite pressure in the cavity. On the other hand, if a finite permanent pressure appears, the mold will always show a permanent deflection, without necessarely producing flash. The permanent pressure level will increase with higher applied packing pressure, but with a thin gate a high packing pressure will not automatically imply a permanent finite pressure and mold deflection. All it comes to, is the fact that the packing efficiency, quantified by the final volumetric shrinkage, is related to the effective internal packing pressure, the duration of the compensating flow (which drastically depends on the gate thickness), and the frozen skin thickness (which relates to the filling rate).

With a thick gate (gateless configuration) the packing pressure is applied until total freeze of the parts core. As long as the internal pressure is present, the mold is in the deflected shape. At the end of packing the part is totally frozen and the shrinkage that follows is small (no phase change). Shrinkage will normally bring about the mold deflection relaxation. But in this case, the shrinkage is so small that only partial relaxation of the deformation can occur and a non-zero internal pressure limit is reached at the end of the cycle, i.e., a permanently deformed cavity. If we use the same processing conditions with a thin gate, thermal sealing will interrupt the compensating flow, leaving a significant molten core section. This liquid will undergo a high shrinkage during the phase change, permitting total relaxation of the mold deformation and no permanent pressure and deflection.

When using a thin gate, the fill rate will influence the onset of mold elasticity assisted overpacking. Assuming a given gate freeze-off time, independent of the fill rate (this is not totally correct), filling the part slowly will give a thick frozen skin at fill time, and therefore less shrinkage. This means that for a given thin gate and packing pressure, overpacking should be more severe at low fill rate. Indeed, going back to *Table 1*, one sees that at 50 mm/s, despite the improved packing efficiency (according to *Table 3*), there is no overpacking for the 0.5 and the 1 mm thick gates.

Trying to correlate the experimental observations with the interpretation based on mold elastic deformation, we modeled the end of the cycle (the packing and cooling) starting from the total freeze of the core section. This means that the following numerical approach is a fairly good representation of the thick gate situation (pressure applied until total freeze), which is the one of interest with respect to residual pressure. The equation of state, representing PVT behavior, is the one used by the MFL (Moldflow) programs:

$$V = \frac{m_1}{m_4 + P} + \frac{m_2 T}{m_3 + P} \qquad \text{(molten state)} \qquad (1)$$

$$V = \frac{s_1}{s_4 + P} + \frac{s_2 T}{s_3 + P} + s_5 \exp(s_6 T - s_7 P) \qquad \text{(solid state)} \qquad (2)$$

$$P = b_1 + b_2 T \qquad \text{(molten/solid boundary equation)} \qquad (3)$$

For our HDPE the coefficients are:

$m_1 = 5522640$

$m_2 = 151.5060$

$m_3 = 1.4761000E + 08$

$m_4 = 4.8937001E + 09$

$s_1 = 4617882$

$s_2 = 154499.7$

$s_3 = 7.8457727E + 11$

$s_4 = 4.4154865E + 09$

$s_5 = 1.2865387E - 07$

$s_6 = 5.0391793E - 02$

$s_7 = 1.0079154E - 08$

$b_1 = -8.1676986E + 08$

$b_2 = 5730156$

These coefficients fit the data when using (Pa), (m^3/kg) and (°C).

Note that this is a purely mathematical fit with no physical meaning and therefore we neglected to mention any physical units for the coefficients. The data have been obtained using a Gnomix apparatus (Prof. Zoller, Colorado).

Our modeling starts at core freeze; therefore we'll use the equation of state (*Eq 2*) only. To model the effect of the mold elasticity, we assume that the increase in volume of the cavity is proportional to the internal average pressure. We start the analysis at the moment the core reaches no-flow (140°C, as measured by Moldflow on this grade).

Because there is no more flow (no heat convection), we can safely average the temperature profile across the thickness and apply the Fourier equation to predict the subsequent cooling history of the material assum reasonable boundary conditions at the mold wall.

Table 3. Actual Maximum Packing Pressure (First Transducer) for Various Geometries and Processing Conditions.

Fill Rate (mm/s)	Gate Thickness (mm)	$P_{nom.}$ 500 Bar	$P_{nom.}$ 800 Bar
5	2	340	600
	1	290	560
	0.5	100	400
10	2	335	610
	1	300	560
	0.5	150	440
50	2	345	620
	1	300	560
	0.5	170	500

This average temperature $T(t)$ has been approximated by an exponential decay. Applying *Eq 2* we have

$$V = \frac{s_1}{s_4 + P(t)} + \frac{s_2 T(t)}{s_3 + P(t)} + s_5 \exp(s_6 T(t) - s_7 P(t)) \qquad (4)$$

if $V = V_0$ one can compute $P(t)$ from $T(t)$ numerically.

The pressure decay we obtain is virtually identical to the Moldflow computed pressure history, both predicting a decay to ambient pressure much faster than experimentally observed. Having verified this limiting case, we introduced mold elasticity, k, by stating that the volume of the cavity is now variable with the pressure:

$$V = V(P(t)) \approx V_0(1 + kP(t)) \qquad (5)$$

Substituting this into *Eq 4*, one gets a new implicit equation for $P(t)$ that we solved numerically. *Figure 11* shows the slower pressure decay due to the mc elasticity. This elasticity coefficient k has been expressed in relative volume increase under a standard pressure of 100 MPa or 1000 bar. The results indicate

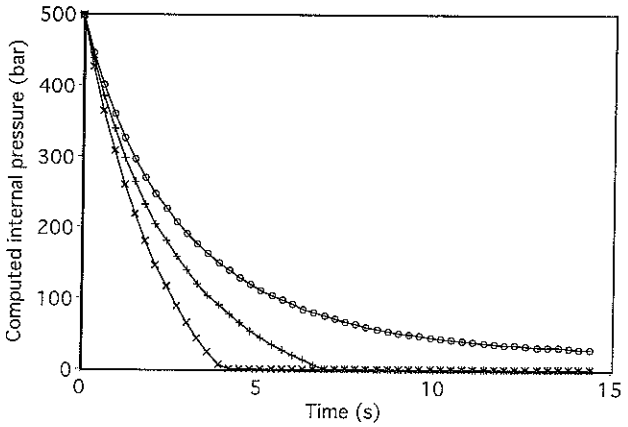

Fig. 11. Numerically computed pressure decay in the cavity for an initial pressure of 500 bar at core freeze, taking into account the mold elasticity. (×) rigid mold, (+) 0.5% vol/1000 bar deformability, and (○) 1% vol/1000 bar deformability.

that at $k \approx 1\%$ vol/1000 bar elasticity and an initial pressure at core freeze of 500 bar, a non-zero permanent pressure, i.e. overpacking, appears. If we express the volume change in terms of average thickness increase of the cavity, this corresponds to ~20 μm, >1000 bar. This order of magnitude has been compared both to the deflection measurements and to analytical estimates.

The strain gauge only quantifies the flexural component of the total deformation, which certainly contains a compressive term as well. Moreover, this gauge is mounted on the back of the cavity plate, which is ~10 cm thick. Based on simple beam assumptions, this flexural strain corresponds to ~15 μm thickness increase. The analytical beam-based estimate yields a similar result (13 μm due to bending and ~7 μm due to uniaxial compression).

Of course, the sample thickness must reflect this situation. The nominal thickness of the cavity has been measured at room temperature to be 2.050 mm, to account for a typical 2.5% linear shrinkage. If we go through the various experiments (different packing pressure for each gate thickness, we find that the permanent pressure and associated mold deformation appears >1100 bars for the thin gate, ~750 bar for the 1 mm gate and at ≈600 bar for the thick gate.

Comparing with *Figs. 4a–4c*, we find these pressure levels to correspond consistently to the levels at which the 2.05 mm thickness is reached, which, by definition, is the onset of overpacking. Higher applied pressures give higher mold deformation and permanent pressures, which result in thicknesses in excess of the actual cavity depth.

In summary, the mold elasticity increases the packing efficiency (7, 8) by storing energy in the wall deformation and using it subsequently to further pack the entrapped polymer (gate sealed). This obviously lowers the theoretical overpacking pressure threshold.

CONCLUSIONS

The cavity we used in this experiment was primarily designed to assess the predictive quality of numerical simulations. The mold performed in an acceptable way when validating the pressure drop in the filling phase.

These experiments mainly point out the difficulty in modeling of the frozen skin growth, given the little knowledge of real transient thermal fluxes (22) and the critical definition of the no-flow temperature (23).

When we started looking at packing phase predictions, we observed significant deviations that we could not explain solely by poor account of thermal fluxes. Indeed, further instrumentation of the mold with a strain gauge has shown the unexpected importance of mold elastic deformation on the internal pressure readings in the packing phase. We decided to conduct the experiment described in this article, focusing on the variables most likely to affect packing efficiency (gate size, packing pressure, time, and filling parameters).

We limited ourselves to thickness measurements to assess average shrinkage, which proved to be a sensible choice. Based on simple elastic deformability of the cavity, our numerical approach yielded predictions of the overpacking and permanent deformation effect in reasonable agreement with the semi-quantitative measurements of the mold deformation in conjunction with the simple analytical estimates.

The systematic experiment conducted here clearly indicates the importance of the gate thickness and the molding machine settings on the shrinkage uniformity and thus on the internal stress level. As we saw, the frozen skin developed at the filling stage can be of great importance for the subsequent packing phase, particularly when using thin gates, a common practice for technical applications parts. The simulation shows some weakness in that area. When the thermal flux and skin-growth modeling have sufficiently improved the commercial codes, it may be worth including mold deformation in the models to yield more realistic shrinkage predictions.

REFERENCES

1. V. Leo and Ch. Cuvelliez in *Injection Moulding of Thermoplastics: Practical Use of Numerical Simulation*, TI KVIV Seminar, Antwerp, Belgium (April 1994).
2. T. S. Chung, *J. Polym. Eng.*, **8,** 175 (1988).
3. H. H. Chiang, C. A. Hieber, and K. K. Wang, *Polym. Eng. Sci.*, **31,** 116 (1991).
4. C. A. Hieber, G. Vandenengel, and H. H. Chiang, *SPE ANTEC Tech. Papers*, **32,** 181 (1986).
5. D. C. Paulson, *SPE ANTEC Tech. Papers*, **16,** 435 (1970).
6. J. Greener, *SPE ANTEC Tech. Papers*, **31,** 822 (1985).
7. B. Miller, *Plast. World*, **49,** No 10,20 (9/1991).
8. A. Cui, M. Konno, N. Nishiwaki, S. Hori, and M. Inoue, *Polym. Process. Soc. Annual Meeting 9*, Manchester, Britain (1993).
9. A. A. Flaman, *Polym. Eng. Sci.*, **33,** 193 (1993).
10. A. A. Flaman, *Polym. Eng. Sci.*, **33,** 202 (1993).
11. K. M. M. Jansen, *Intern. Polym. Proc.*, **IX,** 1, 82 (1994).
12. Ch. Cuvelliez, V. Leo, C. Friedl, and P. Kennedy, *SPE ANTEC Tech. Papers*, **39,** 1618 (1993).
13. H. Recker and G. Menges, *SPE ANTEC Tech. Papers*, **28,** 327 (1982).
14. C. L. Thomas, A. A. Tseng, A. J. Bur, and J. L. Rose, *SPE ANTEC Tech. Papers*, **39,** 143 (1993).
15. J. P. Trotignon and J. Verdu, *J. Appl. Polym. Sci.*, **34,** 1 (1987).
16. *Injection and Compression Molding Fundamentals*, A. I. Isayev, ed., Marcel Dekker (1987).
17. P. Thienel, Th. Droste, and A. Kruse, *Kunststoffe*, 83, **4,** 283 (1993).
18. R. Wimberger-Friedl and J. G. De Bruyn, *Polym. Eng. Sci.*, **33,** 383 (1993).
19. V. Leo, in *"Flow and Cure of Polymers: Measurements and Control,"* RAPRA Seminar, Telford, U.K. (March 1990).
20. M. Saiu, V. Brucato, S. Piccarolo, and G. Titomanlio, *Intern. Polym. Proc. VII*, **3,** (1992).
21. Kistler technical brochure, Piezo Instrumentation, Measuring Instruments for Plastic Processing (1993).
22. C. J. Yu, J. E. Sunderland, and C. Poli, *Polym. Eng. Sci.*, **30,** 1599 (1990).
23. G. Titomanlio and S. Piccarolo, *J. Appl. Polym. Sci.*, **35,** 1483 (1988).

Revision accepted July 1995